Laser Shock Peening to enhance stress corrosion cracking and corrosion fatigue resistance in marine aluminium alloys

J. Kaufman[1,2], M. A. Steiner[3], S. R. Mannava[3], V. K. Vasudevan[4], J. Brajer[2], J. Pilař[2], L. Pína[1], T. Mocek[2]

[1] Faculty of Nuclear Sciences and Physical Engineering, CTU in Prague, Czechia
[2] HiLASE Centre, Institute of Physics of the Czech Academy of Sciences, Czechia
[3] Mechanical and Materials Engineering Department, University of Cincinnati, USA
[4] Department of Materials Science and Engineering, University of North Texas, USA

Abstract
This paper shows the effects of Laser Shock Peening (LSP), an alternative to Shot Peening, on marine aluminium alloys. LSP generated compressive residual stresses which varied depending on the peening strategy and method of confinement. Electrochemical tests indicated a region of increased passivity samples without protective coating as well as significantly reduced intergranular corrosion rate. 3-point bend tests showed significant improvement in fatigue strength. Slow strain rate testing showed strong work hardening of treated specimens although the influence on IGSCC was not clearly indicated.

Keywords marine aluminium alloys, laser shock peening, intergranular corrosion, sensitization

Introduction

5xxx series aluminium alloys are high strength-to-weight ratio weldeable materials known for their exceptional performance in extreme environments such as seawater. They are commonly used in the marine industry for the construction of hulls and other ship-related structures due to their excellent corrosion resistance. The 5xxx aluminium series can also be referred to as aluminium-magnesium alloys due to high magnesium content which is responsible for the enhanced strength. However, when exposed to elevated temperatures (<50 °C) for prolonged periods of time (years), the alloys become sensitized which makes them susceptible to intergranular corrosion (IGC) [1]. Combined with the tensile loading experienced during the ship operation, the IGC can lead to intergranular stress corrosion cracking (IGSCC) [2] and corrosion fatigue (CF) [3] which can result in catastrophic failures. For example, as of 2015, more than 6000 SCC and CF cracks have been documented across the whole Ticonderoga class fleet [4]. Several approaches were tried to address the problem, mainly through metallurgy and electrochemical inhibition but the results were unsatisfactory. In this work, we investigate the stress removal option where tensile stresses in critical areas are replaced with compressive stresses using LSP. While the positive effects of LSP on SCC [5] and CF [6] are well documented using other materials. Studies conducted both with [7] and without protective coating [8] indicate that LSP could also have a direct positive effect on corrosion behaviour.

Experimental methods

For residual stress (RS) measurements, a 6.35 mm thick plate of AA5083-H116 was sectioned using electric discharge machining into 40 mm x 40 mm square coupons. The chemical composition of the alloy is shown in Table 1. The coupons were peened in their received condition without any additional heat treatment. The corrosion fatigue samples were in the form of 60 mm x 12 mm x 4 mm blocks sectioned from a 25.4 mm thick rolled plate. And finally, the slow strain rate test (SSRT) were also sectioned from a 25.4 mm thick rolled plate with dimensions showed in Fig. 1. Both the CF and SSRT were sensitized at 100 °C for 60 days prior to the LSP treatment. The sensitized material was determined to be IGC susceptible following the ASTM G67 standard [9] where the degree of sensitization (DoS) was determined to be 5 mg/cm^2 and 44.6 mg/cm^2 for the as-received material and the sensitized material, respectively.

Table 1 : Chemical composition of AA5083-H116.

Alloy element	Mg	Si	Mn	Fe	Other (Zn, Cr, Ti, Cu)	Al
Composition in wt%	4.0–4.9	0.4	0.4–1.0	0.4	0.65	balance

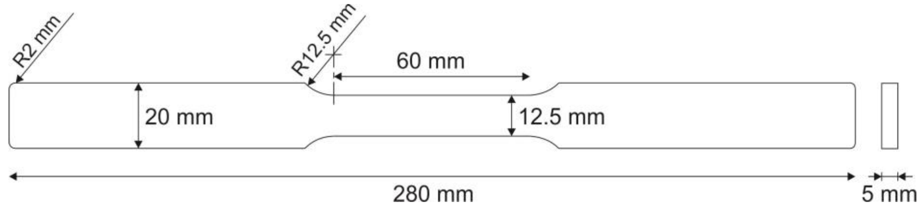

Figure 1 : SSRT sample dimensions.

RS measurements were conducted on an X-ray diffractometer Proto LXRD instrument using the $\sin^2\psi$ method using Cr K_α (2.2897 nm) radiation at $2\Theta = 139°$. To measure residual stresses through depth, layers of the material were progressively removed using an electro polisher with 87.5:12.5 vol% $CH_3OH:H_2SO_4$ electrolytic solution. Corrosion fatigue tests were performed on Electromagnetic pulsator Testronic for high cycle fatigue testing. The 3-point bend test was load controlled and took place at room temperature at 45 Hz with R value 0.1. The supports were 20 mm apart and the specimen was submerged in 3.5% NaCl solution. The terminating condition was either when 10^7 cycles were reached, or when the frequency dropped by 20 Hz due to lowered toughness, signified by a crack that developed and started to propagate. The tensile testing was performed on Kappa 100 SS-CF electromagnetic creep testing machine with a uniaxial strain rate of 10^{-6}. The samples were placed into a specially designed cell which contained circulating 3.5% NaCl water solution kept at constant 40 °C. Prior to the test, the upper and lower wide parts of the specimen were coated with silicon to ensure that only the gauge was in contact with the electrolyte.

The LSP process uses high-energy nanosecond laser pulses to generate deep compressive residual stresses in metallic materials. The sample surface is usually covered with a protective coating in the form of black vinyl tape or paint, which absorbs the focused laser pulses (Fig. 2). The subsequent rapidly expanding plasma is confined against the sample surface by a thin water layer (1–2 mm thick), and a strong shock wave with a magnitude of several GPa [10], is formed. If the pressure exceeds the yield strength of the material, the surface is plastically deformed, and compressive stresses are generated. With the protective coating applied, LSP can be considered a cold working process since the heat associated with the laser absorption is screened from the sample surface and only plastic deformation takes place. In Laser Peening without Coating (LPwC), the surface is directly affected by heat, which can substantially affect the residual stresses in the near surface layer. All samples were peened using first power pre-amplifier of Yb:YAG laser system Bivoj operating at 1030 nm with 10 Hz repetition rate [11] and second harmonic generation option for 515 nm. The laser pulses were 14 ns long with a rectangular temporal and spatial profile with top-hat intensity distribution. Two peening conditions were investigated, one where protective coating was applied while using infrared laser (LSP IR) and second with no protective coating applied while using green laser wavelength (LPwC SHG). The LPwC SHG treatment took place underwater in a water tank. The LSP IR condition used pulses of 3 J focused to a 2.6 mm square laser spot with resulting power density of 3.17 GW/cm^2. The sample after peening is shown in Fig. 2b. When compared to the non-peened sample (Fig. 2a) The surface is clearly deformed but it retains its polished appearance. The LPwC SHG treatment used 1 J laser pulses with laser spot size of 1.5 mm, power density of 3.17 GW/cm^2 and pulse density of 1089 p/cm^2. The LPwC SHG sample after treatment is shown in Fig. 2c. As opposed to the LSP IR sample, a white recast layer was created on the surface.

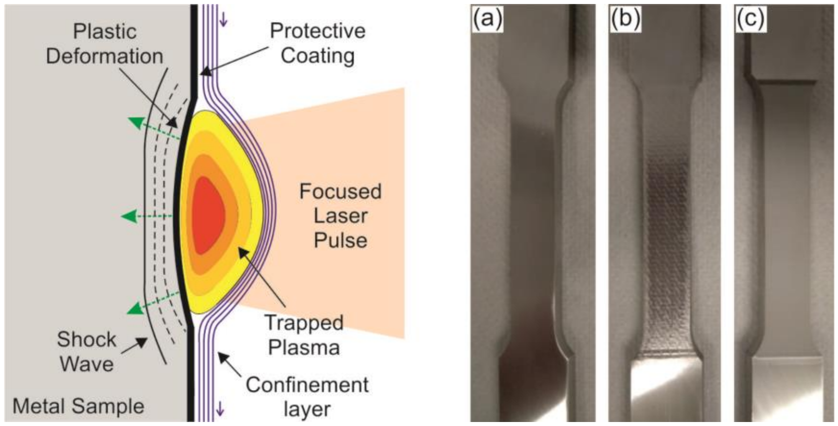

Figure 2: *(left) LSP mechanism and (right)* SSRT samples with (a) no laser peening, (b) LSP IR and (c) LPwC SHG.

Experimental results

Fig. 3 shows in-depth residual stress measurements. Both directions of measurement are shown, that means σ_S and σ_T which represent the scanning and transversal directions, respectively. In comparison with the baseline, the LSP IR treatment with protective tape generates significant compressive residual stresses, around -200 MPa on the surface, with maximum compressive stresses reached at a depth of about 200 µm. The stresses induced in both σ_S and σ_T directions are very similar and no significant variations are observed. The compression depth in both directions is about 1.5–1.6 mm, which is higher than in the LPwC case.

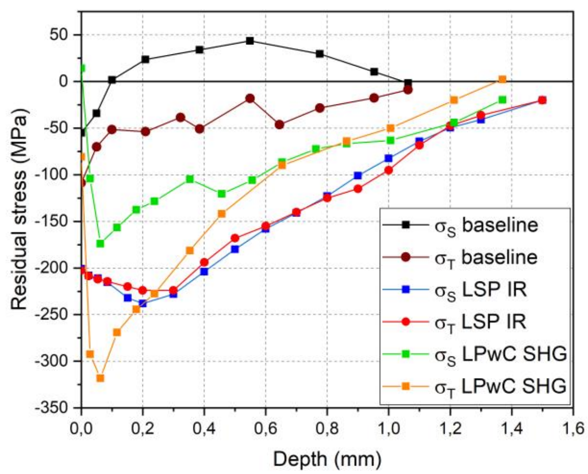

Figure 3: In-depth residual stress measurement where σ_S and σ_T denote stresses in scanning and transversal directions, respectively.

Unlike the LSP IR plots, the LPwC SHG treatment shows a clear distinction between σ_S and σ_T. In scanning direction, the maximum compressive stress reached is 180 MPa and the compression depth is about 1.4 mm. In the transversal direction, the stress curve changes with a maximum compression of about 325 MPa. Similar resultant stress anisotropy with LPwC treatment was observed in other studies. Correa et al. [12] explain the phenomenon in the context of interacting stress fields created by laser pulses overlapping in zigzag scanning patterns.

During SSRT, sensitized samples without any additional treatment were tested first both in air and NaCl solution to determine what effect the environment has on the tensile properties of the samples. The stress/strain curves are shown in Fig. 4a. We can therefore conclude that the decrease in maximum stress and strain to failure is a direct result of the environmental influence of the NaCl solution on the sensitized material. The results of SSRT of sensitized specimens after LSP and LPwC treatments are shown in Fig. 4b. It is immediately clear the material was cold worked by the laser treatment, resulting in its strengthening and raising of maximum stress before breaking. At the same time, the strain hardening lowered the ductility as the nominal strain at break decreased significantly. The maximum stress at failure was achieved with the LSP IR condition with ~8% increase when compared to the baseline although the strain at break dropped by 45%. LPwC SHG had a similar increase in maximum stress of 6% but the strain at break decreased by 18% only.

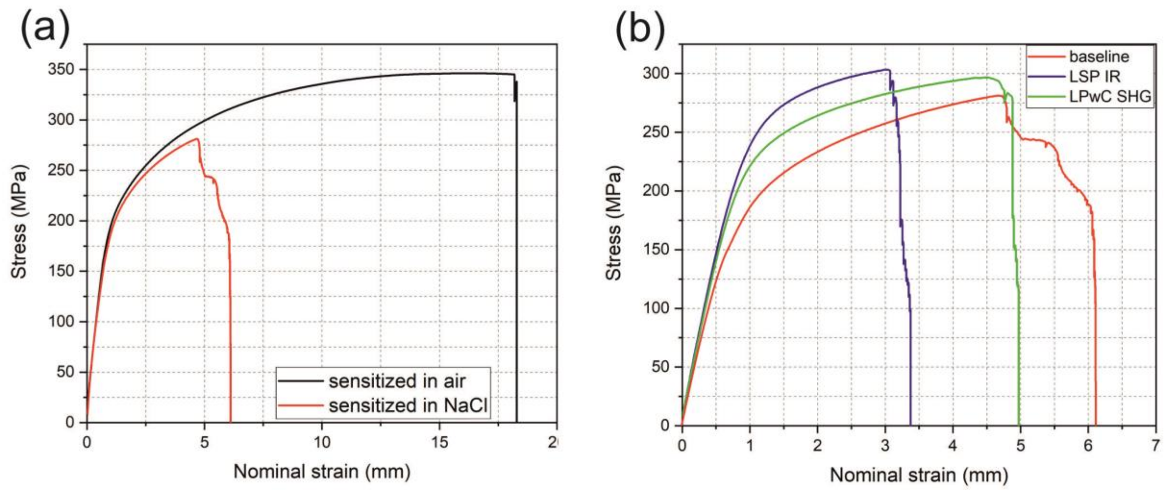

Figure 4: Stress/strain curves of (a) sensitized samples in air and 3.5% NaCl solution and (b) of sensitized samples in 3.5% NaCl solution after LSP and LPwC treatments.

The fracture analysis consists of SEM followed by metallography analysis. All the images are displayed in Fig. 5 to allow for direct comparisons between different sample conditions. The SEM show two different crack propagation mechanisms. Sensitized samples in air show transgranular crack features while all sensitized samples in NaCl show distinct intergranular cracking. The metallographic analysis further reveals that cracks in the NaCl solution were initiated at the specimen surface, specifically at the edges. At first, the intergranular cracks propagated perpendicular to the applied stress due to material weakening in the corrosive environment. As the cracks progressed, the fracture morphology changed to ductile until the specimens fractured completely. Furthermore, as the primary crack propagated, secondary intergranular corrosion cracks split off into the specimen volume. Moreover, next to the primary crack, smaller perpendicular cracks can be observed on the edge surfaces of specimens in NaCl solution which lead to weakening of specimen cross-section. The size and length of these smaller cracks varied among different testing conditions. The cracks were smaller in the LPwC SHG case. This assessment, however, is very rough since laser treated strain hardened specimens failed sooner than non-treated specimens and the surface cracks did not have the same amount of time to develop. Nevertheless, LSP IR specimens with about half the time to failure displayed side intergranular cracks about twice as short which implies linear propagation of the surface cracks in time. Based on this estimate and longer times to failure, we would expect longer surface cracks for the LPwC specimen compared to the LSP IR but the crack length was in fact shorter.

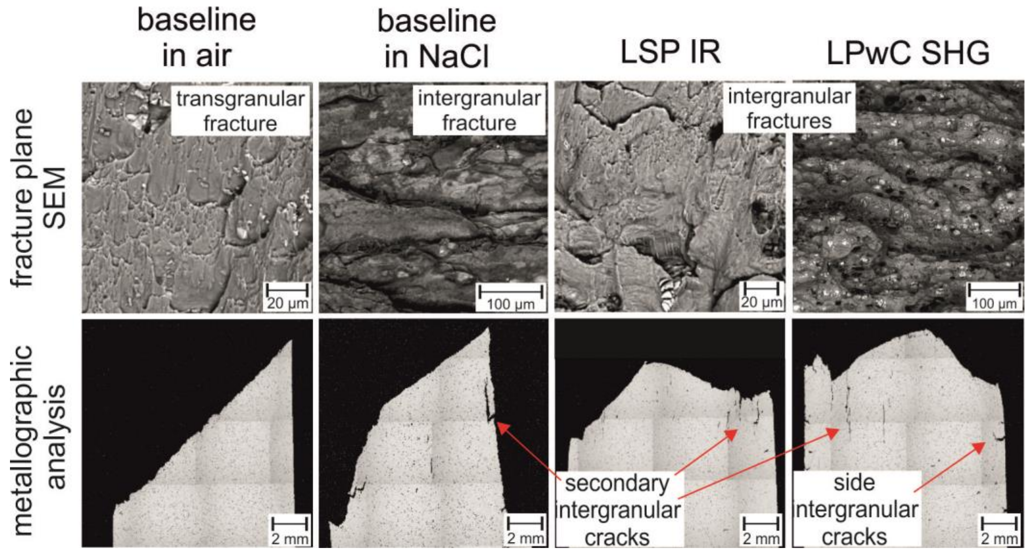

Figure 5: Fracture analysis results.

The results of the 3-point bend test are shown in Fig. 6. The sensitized sample displays the S–N curve shifted down compared to the as received sample which shows a clear negative effect of IGC on the CF of AA5083. The fatigue strength of the non-sensitized baseline material was 127 MPa which is 44 MPa higher than the sensitized baseline sample. Both the LSP and LPwC treatments had a positive impact on the fatigue, bringing the S–N curves back up and possibly improving the original non-sensitized fatigue strength. Better improvements were achieved with the LPwC SHG treatment where the fatigue strength improved by 69%. LSP IR showed lower 59% improvement, but still reached a slightly higher fatigue resistance than the non-sensitized sample.

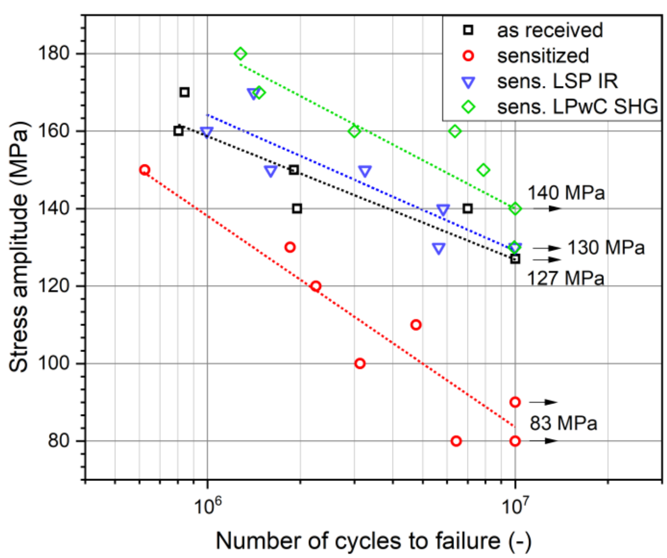

Figure 6: S-N curves of sensitized AA5083 after 3-point bend test in 3.5% NaCl solution

Prior to laser treatment, the effect of sensitization in terms of thermodynamic stability was evaluated by potentiostatic polarization measurement. In order to suppress the chloride driven attack, the samples were polarized at - 800 mV vs Ag/AgCl. The current density measured over time is shown in Fig. 7a. After some time, the current density of the sensitized samples starts rising exponentially, reaching a value of 330 μA/cm^2 over a period of 6 h. On the contrary, the current density of the as received sample stays close to zero and does not deviate over time. The as received and sensitized sample surface after the polarization is shown in Fig. 7b and Fig 7c, respectively. The IGC is clearly visible on the sensitized sample while no pitting is present. When it comes to the treated samples, LPwC SHG treatment shows significant improvement. The current density after 6 h is 5 μA/cm^2, which is nearly the same as that of the as received sample. LSP IR sample with protective coating showed only a slight improvement with final current density of 267 μA/ cm^2.

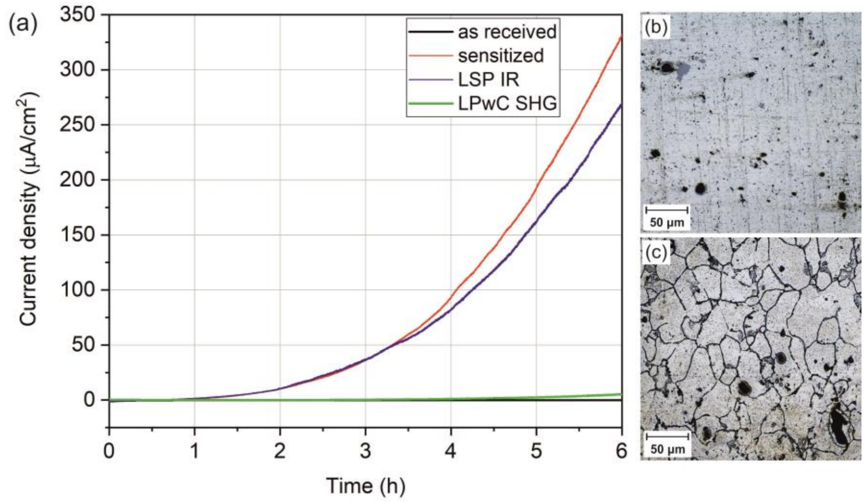

Figure 7: (a) Current density during potentiostatic polarization at -800 mV vs Ag/AgCl electrode of non-treated and treated AA5083 in 3.5% NaCl solution. (b) as received and (c) sample surface after 6 hours of potentiostatic polarization.

Conclusions

In this work, the effect of LSP and LPwC treatment on intergranular stress corrosion cracking and corrosion fatigue of sensitized AA5083-H116 was investigated. Two laser peening configurations were used, one with protective overlay and one without which were further separated by different water confinement. The following conclusions can be made:

1. Both LSP and LPwC imparts deep compressive residual stresses into the studied material. Residual stress anisotropy was observed in the case of LPwC treatment, where larger compressive stresses were measured in the laser advancing direction with respect to the peening pattern.
2. Laser plasma interaction with the aluminium surface associated with the LPwC process creates a recast layer with a modified oxide layer on top in the treated area. This leads to significantly lower intergranular corrosion rate.
3. Sensitization has a negative impact on corrosion fatigue of the material which manifests as a 35% drop in fatigue strength. LSP and LPwC treatment restored and even possibly improved the original fatigue resistance of the non-sensitized samples.
4. The SSRT measurements clearly showed the cold working effect of the LSP treatment. We have observed an increase in maximum stress but at the same time significant decrease in nominal strain at failure as the samples lost some ductility. The effect of LSP on SCC is not clear but some evidence suggests that LPwC treatment slows down the crack propagation.

References

[1] R. Zhang, S. P. Knight, R. L. Holtz, R. Goswami, C. H. Davies, and N. Birbilis, *A survey of sensitization in 5xxx series aluminum alloys*, Corrosion, vol. 72 (2016), pp. 144–159.

[2] J. L. Searles, I. G. Pelagia, and R. G. Buchheit, *Stress corrosion cracking of sensitized AA5083 (Al-4.5 Mg-1.0 Mn)*, Materials Science Forum. Vol. 396. (2002)

[3] R. L. Holtz, P. S. Pao, R. A. Bayles, T. M. Longazel, and R. Goswami, *Corrosion fatigue of al 5083-H131 sensitized at 70, 100, and 175 c relation to microstructure and degree of sensitization*, in DoD Corrosion Conference (2011).

[4] C. Cavas, *Cracks plague ticonderoga-class cruisers*, Navy Times, vol. 9 (2010).

[5] Y. Sano, M. Obata, T. Kubo, N. Mukai, M. Yoda, K. Masaki, and Y. Ochi, *Retardation of crack initiation and growth in austenitic stainless steels by laser peening without protective coating*, Materials Science and Engineering A, vol. 417 (2006), pp. 334–340, 2006.

[6] M. Abdulstaar, M. Mhaede, M. Wollmann, and L. Wagner, *Investigating the effects of bulk and surface severe plastic deformation on the fatigue, corrosion behaviour and corrosion fatigue of AA5083*, Surface and Coatings Technology, vol. 254 (2014), pp. 244–251.

[7] H. Wang, C. Ning, Y. Huang, Z. Cao, X. Chen, and W. Zhang, *Improvement of abrasion resistance in artificial seawater and corrosion resistance in NaCl solution of 7075 aluminum alloy processed by laser shock peening*, Optics and Lasers in Engineering, vol. 90 (2017).

[8] U. Trdan and J. Grum, *Evaluation of corrosion resistance of AA6082-T651 aluminium alloy after laser shock peening by means of cyclic polarisation and EIS methods*, Corrosion Science, vol. 59 (2012), pp. 324–333.

[9] *ASTM G67, Standard Test Method for Determining the Suscepti- bility to Intergranular Corrosion of 5XXX Series Aluminum Alloys by Mass Loss After Exposure to Nitric Acid (NAMLT)*, ASTM International (1999).

[10] R. Fabbro, et al, *Physics and applications of laser-shock processing*, Journal of laser applications vol. 10.6 (1998), pp. 265-279.

[11] P. Mason, M. Divoký, K. Ertel, J. Pilař, T. Butcher, M. Hanuš, S. Banerjee, J. Phillips, J. Smith, M. De Vido, *Kilowatt average power 100 J-level diode pumped solid state laser*, Optica 4 (2017), pp. 438–439.

[12] C. Correa, D. Peral, J. A. Porro, M. Díaz, L. R. de Lara, A. García-Beltrán, J. L. Ocaña, *Random-type scanning patterns in laser shock peening without absorbing coating in 2024-T351 Al alloy: A solution to reduce residual stress anisotropy*, Opt. Laser Technol. Vol 73 (2015), pp. 179–187.